RADIO SCIENCE Journal of Research NBS/USNC–URSI
Vol. 69D, No. 7, July 1965

Effect of the Eclipse of 20 July 1963 on VLF Signals Propagating Over Short Paths

J. H. Crary and D. E. Schneible

National Bureau of Standards, Boulder, Colo.

(Received March 1, 1965)

Measurements were made at Hanover, N.H., of the effect of the solar eclipse of 20 July 1963 on the phase and amplitude of two VLF signals propagated over relatively short paths. The skywave signal from NAA, Cutler, Maine, (14.7 kc/s) was reflected once from the *D* region at a point of total optical obscuration. The skywave signal from NSS, Annapolis, Md., (22.3 kc/s) was reflected from a point where the maximum optical obscuration was 88 percent. Changes in the phase and amplitude of the signals during the eclipse ranged from about 40 percent to 100 percent of the diurnal variation. The times of the maximum phase and amplitude effects were used to calculate effective recombination coefficients for the ionosphere. The maximum amplitude of VLF signals occurred before the time of maximum optical obscuration. This can be attributed to a specific source of ionizing radiation above the sun's west limb, which would be uncovered before the optical maximum. The calculated effective recombination coefficient is about 2×10^{-5}. This value is closer to the value of approximately 3×10^{-6}, calculated from theory by Crain [1961] for the nighttime ionosphere, than to Crain's daytime value. Most values of recombination coefficients from previous radio experiments are closer to Crain's daytime values.

1. Introduction

The total solar eclipse of 20 July 1963 provided a rare opportunity for a measurement of the effect of the eclipse on a VLF signal. The phase and amplitude of a VLF signal propagating over a short path are very sensitive to changes in the *D* region of the ionosphere, such as those caused by an eclipse; the sensitivity is considerably less for long paths.

The changes in the phase and amplitude of a VLF signal during an eclipse may be used for several purposes. First, the changes in phase and amplitude may be used to determine the changes in the equivalent phase height of reflection and the changes in the apparent magnitude of the reflection coefficient. The usefulness of these quantities is limited however, since it is difficult to relate them to anything other than the normal diurnal variations. However, the changes in the amplitude and phase may be used to determine a reaction time and perhaps an effective recombination coefficient from parts of the *D* region which affect the signals. These are important quantities, since so little is known about the ionization production and removal processes in the *D* region [Reid, 1964].

The path of total eclipse in the *D* region (60–100 km height) passed about 200 km southwest of NAA, the high power U.S. Navy VLF transmitter at Cutler, Maine, which was at that time transmitting frequency-stabilized signals at 14.7 kc/s. A receiver was set up at the Dartmouth College field site near Hanover, N.H. The strongest skywave signal which arrived at this receiver from NAA came from a single ionospheric reflection in the area of the *D* region in which the sun was totally eclipsed.

In addition, the 22.3 kc/s signal from NSS at Annapolis, Md., was recorded. In this case the sun was only 88 percent eclipsed at the reflection point. Some characteristics of these paths are shown in table 1. An outline map of the paths is shown in figure 1.

TABLE 1. *VLF signals recorded at Hanover, N.H., during the eclipse of 20 July 1963*

Transmitter call, freq.	Location	Path length	Maximum eclipse % mag.	Type of measurement
		km		
NAA *kc/s* 14.7	Cutler, Maine	406	100	Abnormal loop [a]
NSS 22.3	Annapolis, Md	633	88	Normal loop [a]

[a] See section on experimental procedure.

2. Equipment

The equipment used in this experiment was designed to record the phase of VLF Standard Frequency Transmissions relative to the phase of the output of a rubidium vapor frequency standard, and the amplitude relative to a calibration voltage. The antennas were multiturn shielded loops, 1 m square, tuned to the received frequency. The system output was a pair of d-c voltages for each channel, proportional to the amplitude and phase of the coherent signal. Each pair was recorded on a dual-channel chart recorder.

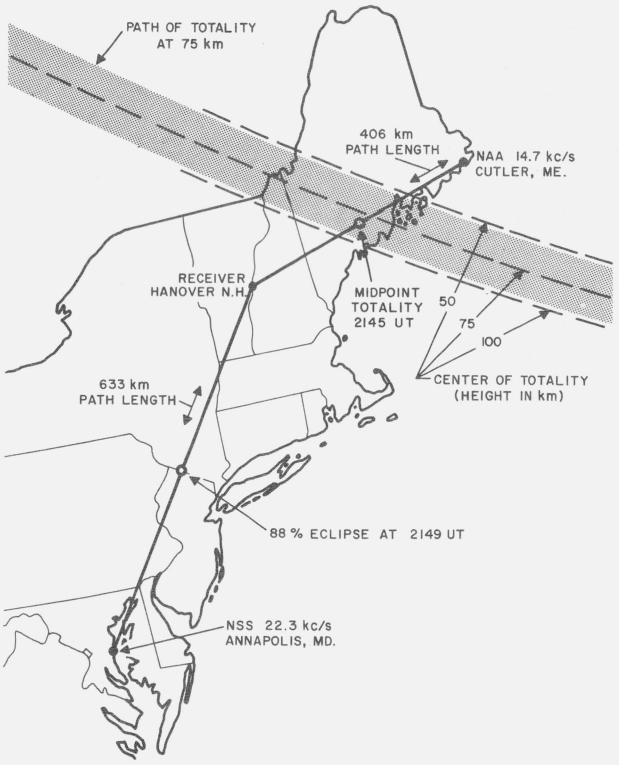

FIGURE 1. *Outline map showing the VLF paths, the time and width of optical totality in the ionosphere, and the times of optical maximum at the reflection points.*

3. Experimental Procedure

It is generally a very good assumption that a VLF transmitter produces only parallel polarized[1] signals. However, some of the parallel polarized energy is converted to perpendicular polarized energy upon reflection from the ionosphere, because of the action of the earth's magnetic field. This reflection may be expressed by the use of the two reflection coefficients $_{||}R_{||}$ and $_{||}R_{\perp}$. The two subscripts indicate the polarization of the incident and reflected ray, respectively [Budden, 1951]. The amplitude of the signal reflected in the parallel polarization is generally several times the amplitude of the converted signal. A normal loop has maximum sensitivity to the parallel polarized groundwave and skywave signals. An abnormal loop has maximum sensitivity to the abnormal skywave [Best et al., 1936].

The ground distance from NAA to the receiver was about 406 km. At this distance, the groundwave is still of greater amplitude than the skywave signal. Since the groundwave is independent of the eclipse effects, it is advantageous to reduce the amount of the groundwave present in the recorded signal. This is often done by taking advantage of the properties of the abnormal loop. The groundwave is initially reduced by rotating the loop to an azimuth perpendicular to the azimuth of the transmitter. A more precise adjustment may then be made by utilizing the fact that the ionospheric signal is minimum at local solar noon [Best et al., 1936]. The loop may therefore be rotated to the point where the signal is a minimum at this time to obtain a position close to the optimum for suppression of the normally polarized signals.

The usual procedure is then to observe the diurnal variation in phase and amplitude and to make incremental changes in the position to determine the optimum orientation. However, it was not possible to observe the diurnal variations for more than a day before, and one or two days after the eclipse. The position obtained by rotating the loop to a minimum at local noon therefore had to be used. Considerable processing of the data is necessary to remove the remaining groundwave component.

4. Measurements

Photographs of the original records obtained during the eclipse are shown in figure 2 following a theoretical curve showing the fraction of the surface area of the sun that is visible at the one-hop reflection point in the *D* region for the NAA–Hanover path. Note that the direction of amplitude increase is downward.

The unobscured fraction of the solar disk was also calculated for the extreme points at the ends of the major axes of the elliptically shaped first Fresnel zone at heights of 60–100 km for both the NAA and NSS signals. The results, shown in table 2, indicate the spread in magnitude of maximum obscuration and times of its occurrence, which would result in an obscuration curve broader than those shown in figure 2

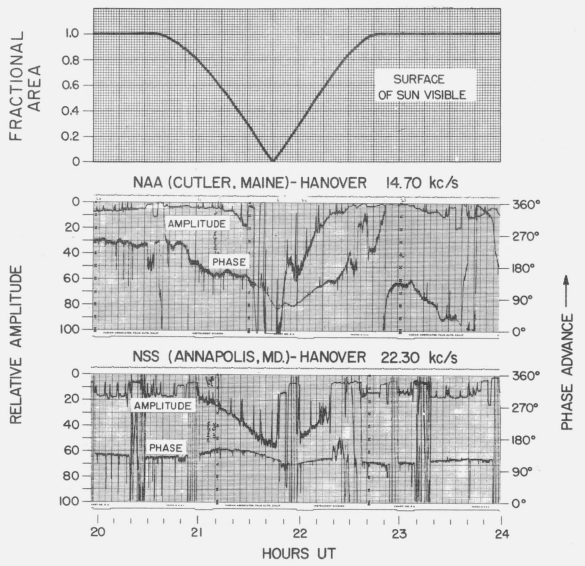

FIGURE 2. *Unobscured fraction of solar disk for NAA reflection point, and VLF records taken at Hanover, N.H., during the eclipse of 20 July 1963.*

[1] The polarization of the signal is called parallel or "normal" when the electric vector is in the plane of incidence, and perpendicular or "abnormal" when the electric vector is perpendicular to it. The terms "normal" and "abnormal" loop refer to a vertical loop antenna oriented with its plane in, or perpendicular to, the plane of incidence of the signal.

for the reflection point. The table shows that, for the NAA reflection area (first Fresnel zone), the times of maximum optical obscuration are spread out over a period of about 2 min, and the unobscured fraction is 0.0142 or less during this period.

The maximum obscuration for the NSS reflection area is spread over about 4 min (−3 to +1 min) around the maximum at 2149 UT at the reflection point. The values of the unobscured fraction deviate up to ±0.04 from the value of 0.12 at the reflection point.

Some characteristics of the equipment should be considered when examining the phase and amplitude records shown in figure 2. First, because both stations were transmitting Morse code traffic, the amplitude was averaged with a time constant of the order of a second or more. The recorded amplitude level of such a signal therefore depends on the average keying rate of the signal. The VLF stations transmitted a short pulse every few seconds for a period of about 3 min in each hour. This is evident on the NAA record in figure 2 at about 49 min after each hour. The average level drops almost to zero during these periods.

Immediately following these pulsing periods, there is a period of continuous (locked-key) transmission; following this is a period of no transmission. The recorded amplitude reaches a maximum and a minimum, respectively, at these times.

The phase scale is shown at the right of each record. When the changing phase reaches zero or 360° at the edge of a chart, it then moves over to the other side of the chart and continues in the same direction. The phase trace generally wanders during the period of no transmission due to noise or a slight unbalance in the system.

It will be noted that the amplitude recording of NAA went off scale during the eclipse. A series of readings of the amplitude were taken independently with other instruments and these values were used where the chart reading was off scale.

Although, unfortunately, NSS was off the air at about the time of maximum effect of the eclipse, a pair of smooth curves were drawn through the available data points for the amplitude and phase, which are believed to represent the actual variation fairly well. The fact that the results for phase and amplitude on both signals are quite consistent indicates that the deduced curves are fairly accurate.

4.1. Removal of Groundwave Components

Polar plots (figs. 3 through 8) were made from the chart recordings after the drift due to the small difference in frequency between the transmitting and the receiving reference oscillator had been removed. A phase advance is counterclockwise in all cases. Relative amplitude from the record origin is shown in units of chart deflection that would be attained for a continuous signal.

In order to obtain the variation of the one-hop skywave signal, it is necessary to correct for groundwave signal present. This may be done by finding a new origin for the polar plot, also shown in the figures, which is close to the origin of the skywave vector. Two methods were used to determine this new origin. The first involved overlaying all the polar plots for a given signal and determining an area within which the skywave origin probably lies. The curvature, the maximum and minimum points, and the overall symmetry of the plot must be considered when using this method.

At the distances involved (400–650 km) the polar plots are complicated by a diurnal phase shift of less than 360°, rapid fluctuations of phase and amplitude

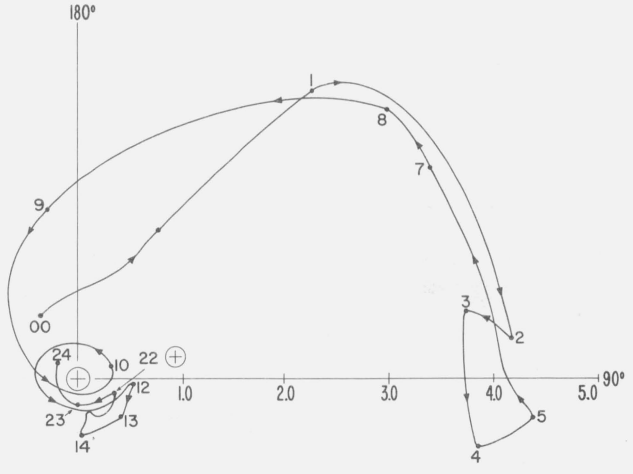

FIGURE 3. *Polar plot of phase and amplitude of NAA (14.7 kc/s) received at Hanover, N.H., 21 July 1963.*

UT is shown on the curve. The scales are drawn to the origin of the original record.

TABLE 2. *Conditions at optical eclipse maximum at heights of 60–100 km for one-hop reflection point and extreme points of first Fresnel zone for paths to Hanover*

Signal	Reflection point		Extreme points of first Fresnel zone							
	UT of max.	% Unobscured	NE point UT of max.	% Unobscured	SW point UT of max.	% Unobscured	NW point UT of max.	% Unobscured	SE point UT of max.	% Unobscured
NAA 14.7 kc/s	2145	0.0	2145	0.00 −.36	2145	1.42 −0.66	2144	0.00 −.40	2146	0.40 −.04
NSS 22.3 kc/s	2149	11.8 −10.7	2146	6.8 −6.0	2150 (60–95 km)	16.3 −15.4	2148	11.5 −10.5	2149	11.5 −10.5

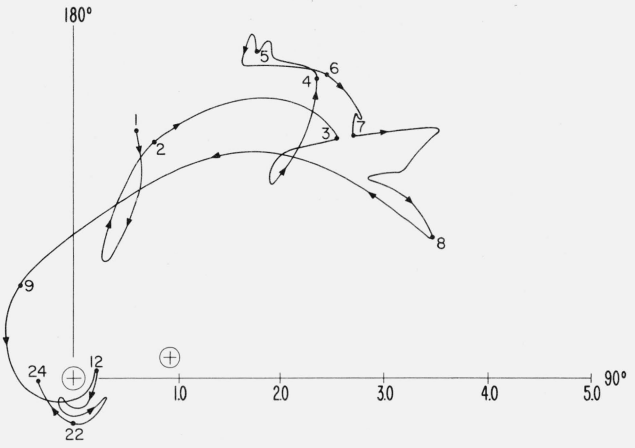

FIGURE 4. *Polar plot of phase and amplitude of NAA (14.7 kc/s) received at Hanover, N.H., 19 July 1963.*

UT is shown on the curve. The scales are drawn to the origin of the original record.

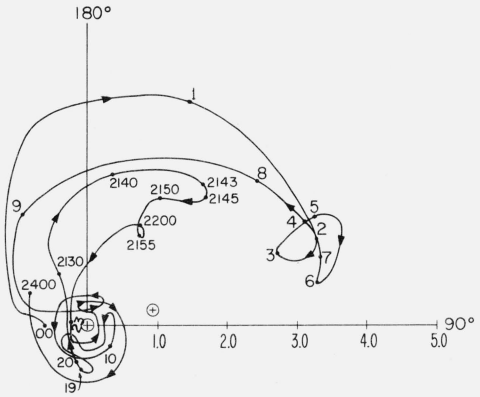

FIGURE 5. *Polar plot of phase and amplitude of NAA (14.7 kc/s) received at Hanover, N.H., 20 July 1963.*

UT is shown on the curve. The scales are drawn to the origin of the original record.

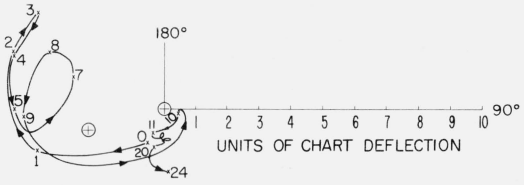

FIGURE 6. *Polar plot of phase and amplitude of NSS (22.3 kc/s) received at Hanover, N.H., 21 July 1963.*

UT is shown on the curve. The scales are drawn to the origin of the original record.

during the night, and disturbance effects. Therefore, a second method was used in conjunction with the first. This method utilizes calculated values of diurnal phase and amplitude changes to determine independently the area of probability for the skywave origin. The

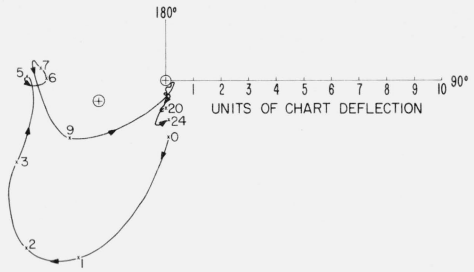

FIGURE 7. *Polar plot of phase and amplitude of NSS (22.3 kc/s) received at Hanover, N.H., 22 July 1963.*

UT is shown on the curve. The scales are drawn to the origin of the original record.

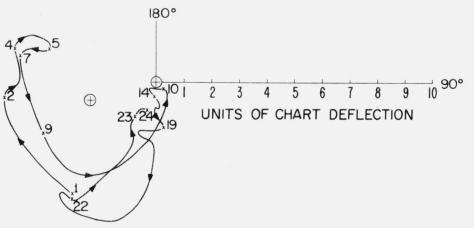

FIGURE 8. *Polar plot of phase and amplitude of NSS (22.3 kc/s) received at Hanover, N.H., 20 July 1963.*

UT is shown on the curve. The scales are drawn to the origin of the original record.

necessary equations and information are given in appendix A.

The use of both of these methods resulted in the choice of another origin which is shown in the polar plots. The magnitude and direction of the displacement from the first origin represents the best estimate of the phase and amplitude of the groundwave vector, or the location of the origin of the skywave vector.

4.2. Results

The linear plots (figs. 9 through 12) were made with the new origin and, it is believed, show essentially the skywave alone. These contain the same information as the polar plots but in a more convenient form.

The amplitude and phase scales used on the linear plots are the same as those used on the original records and in the polar plots. Since the amplitude and phase values normally vary during the 2 hr eclipse period, the midpath noon values averaged over the two control days were used as the reference for the calculations and curves of the eclipse effect.

From the linear plots, the phase change at any time during the eclipse can be determined, and the corresponding change in path length calculated by (2). The height change can then be determined by substitution into (1). By this method, it was determined that the height change during the eclipse reached a maxi-

mum of 10.9 km at the NAA-Hanover one-hop reflection point and 6.85 km at the NSS-Hanover one-hop reflection point.

A ratio of amplitudes and a corresponding ratio of relative reflection coefficients were then calculated from (10) or (11), using the height changes calculated above to compute P_N/P_D. The amplitude ratio is graphically presented for the NAA-Hanover path (fig. 13) and the NSS-Hanover path (fig. 14) for the eclipse period. The average values for the two days of background data, with the bars on the average values giving the range of variation over the two days, are shown for comparison. These figures also show, on the same time scale, the result of calculations of the height change, and the unobscured fraction of the sun's visible surface. The daytime skywave and groundwave from NAA are nearly equal in amplitude and opposite in phase. The resultant signal is small, which causes low amplitude and consequent uncertainty, since the signal is very sensitive to small ionospheric changes. The NSS signal amplitude and phase are such that the time of the NSS amplitude maximum is more sensitive to the position of the new origin than are the times of the other amplitude and phase maxima.

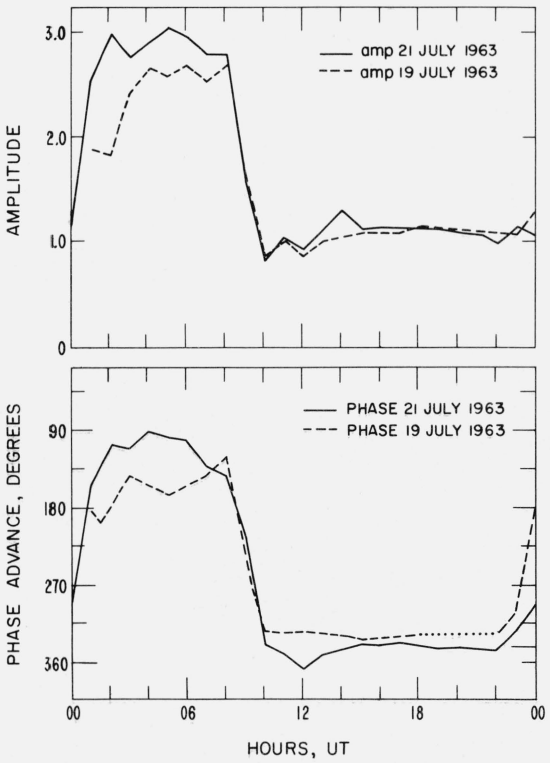

FIGURE 9. *Skywave phase and amplitude of NAA (14.7 kc/s) recorded at Hanover, N.H., plotted with new origin for 19 and 21 July 1963.*

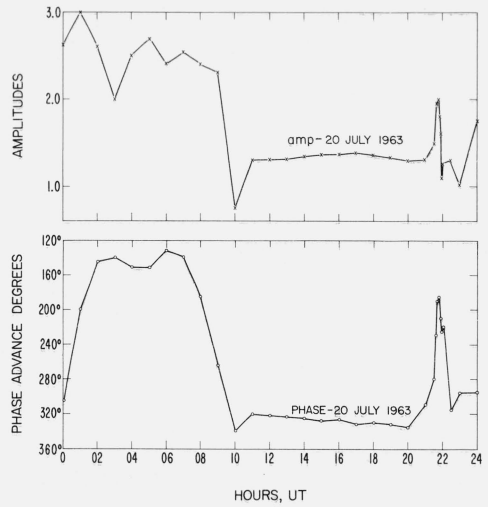

FIGURE 10. *Skywave phase and amplitude of NAA (14.7 kc/s) recorded at Hanover, N.H., plotted with new origin for 20 July 1963.*

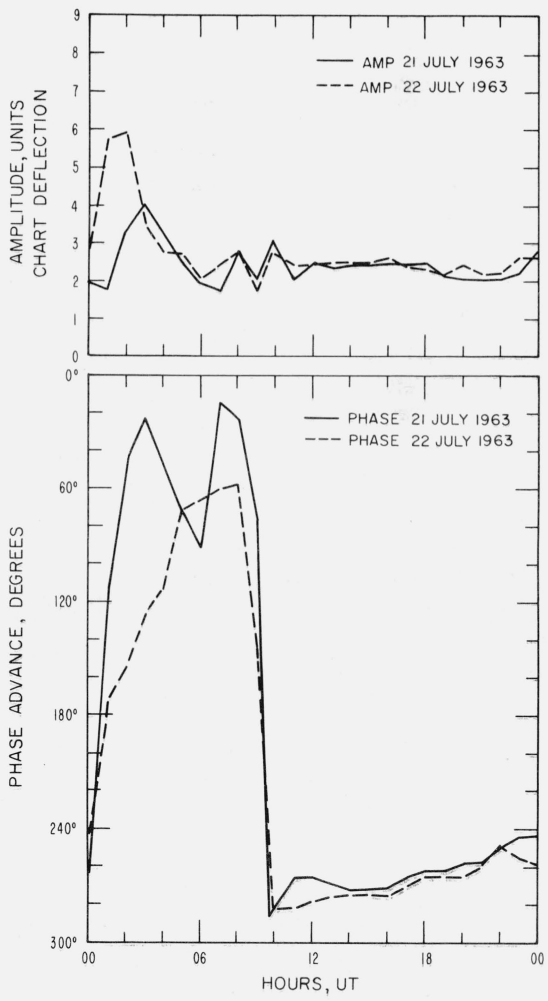

FIGURE 11. *Skywave phase and amplitude of NSS (22.3 kc/s) recorded at Hanover, N.H., plotted with new origin for 21 and 22 July 1963.*

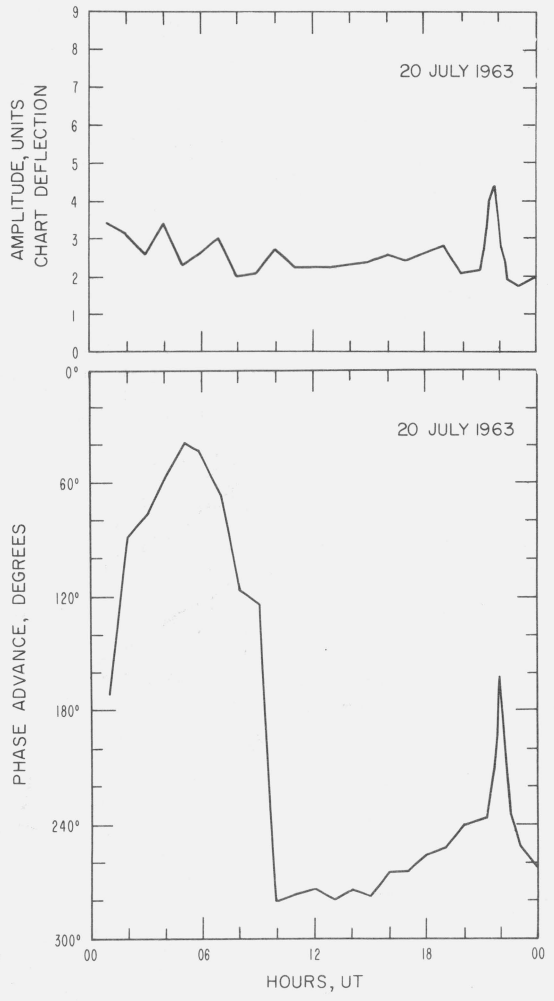

FIGURE 12. *Skywave phase and amplitude of NSS (22.3 kc/s) recorded at Hanover, N.H., plotted with new origin for 20 July 1963.*

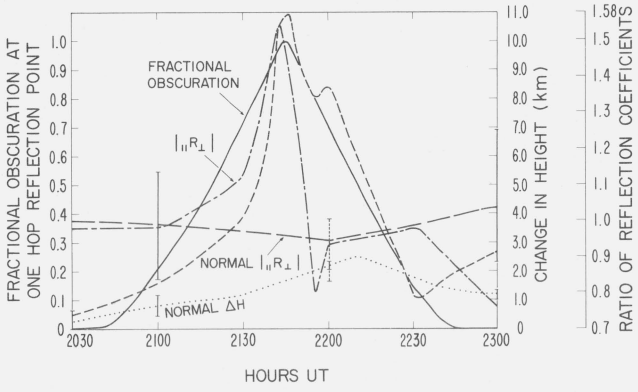

FIGURE 13. *Optical obscuration, calculated height change, and reflection coefficient ratio for NAA signal during the eclipse of 20 July 1963.*

The bars indicate the range of values at these times on the control days.

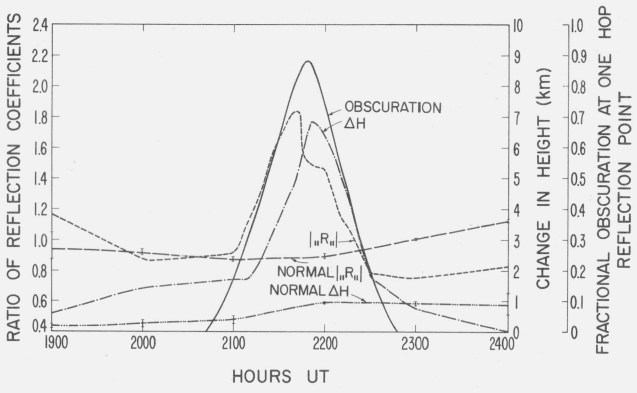

FIGURE 14. *Optical obscuration, calculated height change, and reflection coefficient ratio for NSS signal during the eclipse of 20 July 1963.*

The bars indicate the range of values at these times on the control days.

5. Analysis of Results

The VLF effects of the eclipse measured at Hanover are summarized in table 3. In most cases the changes in magnitude and phase of the reflection coefficients were not as large as the regular diurnal variation. The only possible exception was the change in the apparent magnitude of the reflection coefficient for the 22.3 kc/s signal. The limited amount of data available leaves enough uncertainty about the diurnal variation to make the value of the comparison of the magnitude of the diurnal and the eclipse variations somewhat doubtful. As previously indicated, the origin used yields values which agree approximately with the VLF propagation calculations. However, the magnitude of the deduced diurnal variation is sensitive to the position of the new origin. Equation (5) indicates very little difference in the magnitude of the parallel reflection coefficient, and consequently in the amplitude, for night and day. The data are consistent with this result. It is difficult to draw any conclusions about the meaning of the magnitude of these effects because of the uncertainty about the behavior of the solar radiation versus time, as we shall see later.

One of the most striking features of the eclipse effect is that the maximum signal amplitude occurred considerably before the optical eclipse maximum. The magnitude of these time differences is such that they could not be due only to errors in timing. The probable explanation for these early maxima will be taken up later in the paper.

The changes in the amplitude and phase of the VLF signals during the eclipse are caused by changes in the ionization density in the D region. In the case of the phase of the signal, we may reasonably assume that the signal is reflected from a height at which the ionization density N is approximately 300/cm^3 [Budden, 1953]. The phase then essentially indicates how the height at which this ionization density occurs varies as a function of time. The time at which this height is a maximum corresponds to the time at which a mini-

mum in the ionization density is present at a given height.

The time delay of the phase effect relative to the maximum optical obscuration was used to calculate effective recombination coefficients. These calculations are based upon the following assumptions: (1) The ionizing radiation which affects the phase was a minimum at the time of maximum optical obscuration and; (2) the method of analysis given by Appleton [1953] may be applied here. Appleton assumes an αN^2 type of reaction. This is valid only when the ion to electron density ratio λ is constant, i.e., no attachment type of reaction is present. He shows that for the αN^2 type of reaction, when the electron production rate has an extreme value, the delay time Δt for the extreme value of N is approximately $\Delta t = 1/2\alpha N$, for small Δt, where α is the effective recombination coefficient, and N the electron density. This approximation can be better applied to small delay times as recorded during the eclipse than to larger ones such as during SPA, etc. If λ does not remain constant, Lerfald et al., [1965] show that the times of minimum ionization should not be delayed after the eclipse maximum. The fact that a delay is observed may indicate that λ does remain constant or nearly so. In any case it means that the change in λ does not completely dominate the process.

Using Appleton's expression, and taking the value for the electron density at the reflection point of 300/cm^3 we can calculate the effective recombination coefficient for the regions which affect the phase of VLF signals given in table 3. The results are $\alpha = 2.8 \times 10^{-5}$ for 14.7 kc/s at a height of about 85 km, and $\alpha = 1.4 \times 10^{-5}$ for 22.3 kc/s at 80 to 82 km (based upon the calculated height change and the assumed 74 km daytime height).

Now let us consider the time of the maximum amplitude. The maximum amplitude occurs several minutes before the maximum optical obscuration, especially in the case of the NSS measurements; this time difference is sufficiently large to rule out timing errors as the sole source of the time lead, as mentioned previously.

It appears then that the explanation for the early time of the maximum amplitude lies in some physical effect caused by the eclipse or in some propagation effect. The first explanation that one might consider is that of some sort of interference phenomenon. The actual ionosphere is, of course, much more complicated than the single slab model considered so far. Studies of ionosphere models with exponential ionization profiles, for instance, have revealed very complicated behavior of the reflection coefficient as a function of changes in the profile [Wait and Walters, 1963]. It is possible that such a configuration might produce, merely by interference between partially reflected rays, an interference pattern which has a maximum amplitude at any time. The fact that the maximum amplitude occurred considerably before the optical maximum of the eclipse on both VLF paths makes it seem unlikely that this could be merely a fortuitous interference effect. When the times of occurrence of the maximum amplitude are analyzed further, we shall see that the particular times at which the maximum occurred have a significance which is unlikely to have occurred by mere accident.

Let us then consider another possible explanation for this early time of maximum amplitude. Assume that the ionosphere may be represented, as far as the effect is concerned, by two homogeneous slabs. The lower slab, of arbitrary thickness, has values of electron density and collisional frequency such that it produces only attenuation of a wave passing through it. The upper, semi-infinite slab has the proper electron density and collisional frequency so that it produces a reflection at the lower edge. It is possible that the early time of maximum amplitude then could be caused by some component of the ionizing radiation which affected only those lower heights where the majority of the attenuation, and thus the change in the amplitude or the apparent magnitude of the reflection coefficient, is produced.

The variation in the amplitude is caused by the variation in the ionization density present in part of the D region where the attenuation is produced. The time variation of the amplitude then is indicative of the time variation of the ionization density and the delay time may be treated in a similar manner.

The question of the source of the ionizing radiation immediately comes to mind. Bracewell [1952] has stated that he saw no indication of any effect of the obscuration of active areas on the VLF signals during the eclipse of 28 April 1949. No other mention of this effect in the D region has been found in the literature, although it has been reported in E-region studies [Minnis, 1955; Ratcliffe, 1956].

TABLE 3. *Summary of VLF effects of 20 July 1963 eclipse measured at Hanover, N.H.*

Station, location, frequency, and distance	Solar obscuration		Maximum						
			Magnitude of reflection coefficient ratio			Change of phase and apparent reflection height			
	UT	% Mag	UT	Ratio	% of Diurnal variation	UT	Phase	Height	% of Diurnal variation
							Degrees	*km*	
NAA, Cutler, Me. 14.7 kc/s, 406 km	2145	100	2143	1.54	77	2146	144	10.9	68
NSS, Annapolis, Md. 22.3 kc/s, 633 km	2149	88	2142	1.83	100	2151	102	6.85	43

The ionizing radiation which produces the daytime *D* region is generally considered to consist of Lyman Alpha (1217 Å), x rays of $\lambda < 10$ Å [Nicolet and Aiken, 1960] and cosmic rays [Reid, 1964]. The cosmic radiation should provide a constant ionizing source which will not vary during the eclipse. It appears that at least as a first assumption, cosmic rays will not contribute any asymmetry about the time of maximum eclipse so they will not be considered further. Friedman [1963] found from rocket measurements during the 12 October 1958 eclipse that the Lyman alpha radiation fell to values comparable to the general sky background level, but about 12 percent of the x-ray flux persisted throughout totality. Furthermore, Friedman found that the x-ray intensity in the corona was six times as great on the west limb, which contained several active plages, as on the east limb, which was free of activity.

Another measurement by Friedman [1963] with a rocket-borne pinhole camera in April 1960 showed that the x-ray emission extended about 0.06 solar radii, or 43,000 km, above the solar limb. The examination of available x-ray records and Calcium-K line photos led Friedman to the conclusion that most x radiation comes from the corona above bright plages. A further comparison shows that the x-ray source contours very closely resemble the contours of the 9.1 cm spectroheliograms made at Stanford University [CRPL F–Series 1963].

The optical eclipse is caused by the obscuring of the sun's visible disk by the disk of the moon. These two disks are approximately the same size. It is evident then that an area above the visible solar disk, located at or near the limb of the sun, would extend considerably beyond the visible disk. If it is near the solar equator, it can be eclipsed and uncovered earlier or later than the first or last contact of the optical eclipse, depending upon whether this region was located near the east or west limb of the sun. These considerations suggest the possibility that the eclipsing of active x-ray producing areas above the optical disk should be considered as an explanation for the early time of maximum amplitude.

A map of the sun's surface at the time of the eclipse [Billings et al., 1963] shows that the visible disk covers 312 to 134° heliographic longitude. There was an active 5303 Å emission region located between about 130 and 165°, at latitudes between about 3° S and 12° N. Two calcium plages were noted at 139.5° longitude and 14° N latitude, and 149.5° longitude and 4° N latitude. This region also appears on the 9.1 cm spectroheliogram made at Stanford University at the time of the eclipse. The region would have been at the west limb of the sun. The active x-ray producing area above this region would have been eclipsed before first contact of the optical eclipse, and would have been uncovered before optical maximum.

A rough calculation was made, assuming that (1) the apparent size of the solar and lunar disks are the same, (2) the rate of motion was uniform, and required 2 hr from first to last contact, and (3) the upper limit of 0.06 solar radii found by Friedman is typical for the maximum height of x-ray sources above the limb. The calculations indicated that the region above the plages and active regions should be uncovered 3.7 min and 7.2 min before optical maximum for the NAA and NSS one-hop reflection points, respectively. Let us consider the NAA signal first. The maximum amplitude occurred 2 min before the optical maximum. Therefore, the maximum amplitude occurred about 1.7 min after the calculated time of the uncovering of this active area. The maximum amplitude of the NSS signal occurred about 7 min before optical maximum. Therefore, the maximum amplitude occurred about 0.2 min after the calculated time of the uncovering of the active area. The corresponding delay times for the maximum phase effect on NAA and NSS, respectively, were 1 and 2 min. These delay times all lie close together, with the calculated delay for the amplitude effect on the NAA signal lying in between the two values calculated for the phase effect. This suggests that at least the amplitude delay for the NAA signal is fairly reasonable. As was mentioned before, the time of the NSS signal amplitude maximum is more dependent than the others on the position of the new origin for the polar plot. The fact that the measured time delay is only 0.2 min is believed to be largely due to this fact. In addition, the signal-to-noise ratio of the NSS signal was a bit smaller than that of the NAA signal which contributes a little more uncertainty to the time of maximum.

It is very difficult to determine the magnitudes of the errors involved in the measurement of these time delays. Actual timing errors on the record are expected to amount to not more than ± 0.5 min. The amplitude and phase measured on the record, however, is the result of an effect which is integrated over the area of the first Fresnel zone. The time of optical maximum varies over this first Fresnel zone by about 2 min in the case of the NAA signal and by about double this in the case of the NSS signal. Since the actual contribution of any part of these areas decreases as its distance from the center increases, it is very difficult to set an actual numerical limit on the effects of this variation on the time of maxima. Although the delay times measured on the 22.3 kc/s signal from NSS tend to be a bit higher than those measured for the 14.7 kc/s signal from NAA, there is not sufficient precision available to say that the difference is significant. It is better to find a reasonable average value for the results. As indicated in table 4 this yields a value of approximately 2×10^{-5} for the effective recombination coefficient. It seems very unlikely that the error of the measurement could account for the difference of roughly a factor of ten from many previous values obtained by other observers.

The values determined by others for the effective recombination coefficient are also tabulated in table 4 [Mitra and Jones, 1954]. The other values were not taken during an eclipse but during daytime conditions or during SPA's when λ would be expected to be constant. It should be noted that the delay times found during most of these are quite long, ranging all

the way from $4\frac{1}{2}$ to 80 min. Bracewell [1952] determined that during an earlier eclipse the delay time could be not larger than 6 min. In addition, Bracewell and Straker [1949] stated that the relaxation time determined from SPA's due to solar flares does not exceed 5 min and may be much less. They further state that in at least one case the time is 2.5 min or less. Furthermore, Gallet [1955] found that absorption measurements made during the eclipse of June 20, 1955, yield a time delay of not more than 1 or 2 min. These time delays are very close to the eclipse values determined in this paper and would yield similar effective recombination coefficients.

There is therefore considerable experimental evidence of these high effective recombination coefficients. The values given by Mitra and Jones [1954] bracket the daytime values ($\cong 1 \times 10^{-7}$ at 80 km) shown by Crain. The values calculated here are nearer to the values ($\cong 2 \times 10^{-6}$) given by Crain for the nighttime case. It is also possible that the ionospheric conditions in the *D* region at the eclipse maximum were close to those of nighttime, since the apparent reaction time is about the same as the duration of totality (2 min). These results would be reasonable for the ionosphere about 20 km lower, i.e., 60 km [Mitra and Jones, 1954; Crain, 1961]. It is perhaps more likely that this indicates an attachment type of reaction is actually present, although not dominant.

The reversal of the direction of change of the height and reflection coefficient ratio for the NAA signal and the change in slope of the reflection coefficient ratio for the NSS signal, which occurred several minutes after the optical maximum, could have resulted from the obscuration of some active region. However, these times do not appear to correspond to the covering or uncovering of any obvious feature on the sun. It appears more likely that it is due to a relatively weak interfering signal such as the second order ionospheric reflection.

It seems a little strange at first that there was no noticeable effect on the signals when the x-ray producing area was first obscured a few minutes before optical first contact. The answer probably lies in the fact that the fractional change in radiation was small, since the visible disk and any other x-ray producing areas were still unobscured.

TABLE 4. *Comparison of calculated values of the effective recombination coefficient*

Approx ht.	Method	f	Delay time	αN sec^{-1}	Assumed N	α	Calculated by	Data source
km		*kc/s*	*Min*		*e/cm*^{3}	*cm*^{3}*/sec*		
80	Absorption	150	60	$1.4 \cdot 10^{-4}$	800	$1.7 \cdot 10^{-7}$	Mitra and Jones	Benner
80	Absorption	150	60	$1.4 \cdot 10^{-4}$	600–1200	1.14 to $2.3 \cdot 10^{-7}$	Mitra and Jones	Benner
80	Polarization	150	80	$1 \cdot 10^{-4}$	800	$1.3 \cdot 10^{-7}$	Mitra and Jones	Nearhoof
			80	$1 \cdot 10^{-4}$	600–1200	$1.7 \cdot 10^{-7}$ to $8 \cdot 10^{-8}$		
90	Phase height	150	30	$5.2 \cdot 10^{-4}$	3060	$1.7 \cdot 10^{-7}$	Mitra and Jones	Jones
75	"$D\alpha$" phase ht.	16	25±5	$3.6 \cdot 10^{-4}$	280	$1.3 \cdot 10^{-6}$		Bracewell and Bain
68	SPA decay					$1.9 \cdot 10^{-6}$	Mitra and Jones	Ellison
70	SPA decay					$2.2 \cdot 10^{-6}$	Mitra and Jones	Ellison
73	SPA decay	16				$6.3 \cdot 10^{-6}$	Mitra and Jones	Bracewell
65–75	SPA decay Cls 1–2+ flares mean values	16	8			$3.5 \cdot 10^{-6}$	Mitra and Jones	Mitra and Jones
65–75	SPA decay Cls 3–3+ flares mean values	16	4.5			$6.3 \cdot 10^{-6}$	Mitra and Jones	Mitra and Jones
80–85	Amplitude and phase during eclipse	14.7 22.3	1 2	$\sim 6 \cdot 10^{-3}$	~ 300	$\sim 2 \cdot 10^{-5}$	Crary and Schneible	Crary and Schneible

6. Conclusions

The measuring techniques and the methods used to analyze the VLF records from the eclipse yield results which are consistent with the theories of propagation and the present knowledge of ionospheric conditions during the eclipse. The effective recombination coefficient calculated from these eclipse data is higher by a factor of 10 or more than the values calculated by most experimenters. In addition it is nearer the value calculated from theoretical considerations by Crain for the nighttime *D* region than it is to that calculated for the daytime *D* region. Other observers have obtained values of time delay from eclipse and SPA data which are of the same magnitude as those obtained in this paper. It is possible that the actual heights involved are considerably lower, where the recombination coefficient is greater, but it is more likely that this indicates an attachment type of reaction rather than true recombination [Reid, 1964].

The fact that the NAA amplitude delay time agrees so nicely with the delay times calculated from the phase results indicates that the assumption about the x-ray source is very likely the true explanation. In addition these assumptions are in line with the known facts about the Lyman alpha, cosmic rays and x radiation which are the source of *D*-region ionization.

It is plausible then, that the ionization at the higher heights which affects the phase (say, above 80 km) did result from the Lyman alpha radiation from the visible disk, while the ionization at the lower heights, which affects the amplitude, was caused by the x radiation.

This radiation can reasonably be assumed to arise from the area above the visible disk over an active area at the west limb. This active area was also observed in 5303 Å emission [Billings et al., 1963] and also in the 9.1 centimeter spectroheliograms [CRPL–F Series, 1963] made of the sun around the time of the eclipse.

The authors acknowledge the work of A. H. Diede, who designed and constructed the equipment and was mainly responsible for its operation, and H. M. Burdick, who planned and constructed the mobile installation.

We are indebted to M. G. Morgan of the Thayer School of Engineering, Dartmouth College, Hanover, N.H., for allowing us to use the Dartmouth field site facilities, and further to M. G. Morgan and his staff for the many details with which they aided us.

The authors are also indebted to A. G. Jean and D. D. Crombie for many stimulating ideas and discussions, and to F. M. Malone of the Office of the Chief of Naval Operations, for his aid regarding the VLF transmitters whose signals were used.

The work was partly supported by the Advanced Research Projects Agency, Washington, D.C., under Order 183.

7. Appendix A. Calculation of the Expected Diurnal Changes in Phase and Amplitude

The distance of a single trip between earth and ionosphere is given [Helliwell, 1953] by

$$P^2 = 2R(h' + R)/[1 - \cos(180D/\pi R) + h'^2], \qquad (1)$$

where P = ray path distance in km,
h' = height in km,
D = total ground distance in km,
R = mean earth radius in km.

Then, the expected diurnal phase change is found by substituting the values for the night and day ray path distances into the expression

$$\triangle \phi = \frac{2(P_N - P_D)(360°)}{\lambda}, \qquad (2)$$

where the N and D refer to night and day conditions, respectively. The values of 74 km for the noon reflection height and 16 km for the diurnal change have been indicated by others [Bracewell et al., 1951] and were used here. The change in height for a given phase change is relatively insensitive to the value of height assumed in this range, so the exact value of the height is not critical. The assumed reference height of 74 km is used only to define the height range of the effects being measured.

Determining the theoretical diurnal amplitude change requires two simplifying assumptions. First, it is assumed that the ionosphere is a sharply bounded homogeneous medium with a constant magnetic field; second, that the Q–L approximation is valid [Crary, 1961]. Budden [1951], and Wait and Murphy [1956] give expressions for the refractive indices μ_0, μ_e, and reflection coefficients of such a medium in terms of the parameters ω_r and τ.

Reasonable values of these parameters for the ionosphere for VLF have been determined from experimental data by Wait and Murphy [1956, 1957], Budden [1951], Bracewell et al. [1951], and Crary [1961]. These values are: for night $\omega_r = 5 \times 10^5$, $\tau = 60°$, and $h' = 90$ km; for day $\omega_r = 1.5 \times 10^5$, $\tau = 15°$, and $h' = 74$ km. Then the angle of incidence at the ionosphere, as expressed by Helliwell [1953], is

$$\theta = \tan^{-1}\left\{\sin\left(\frac{180D}{\pi R}\right) \Big/ \left[1 + \frac{h'}{R} - \cos\left(\frac{180D}{\pi R}\right)\right]\right\}. \qquad (3)$$

Budden [1951] gives equations for the reflection coefficients in the form

$$_{||}R_{\perp} = 2i\, C(\mu_0 C_0 - \mu_e C_e)/D \qquad (4)$$

$$_{||}R_{||} = [(\mu_0 + \mu_e)(C^2 - C_0 C_e) + (\mu_0 \mu_e - 1)(C_0 + C_e)\, C]/D \qquad (5)$$

where $\mu_e \sin\theta_e = \mu_0 \sin\theta_0 = \mu \sin\theta$

$D = (\mu_0 + \mu_e)(C^2 + C_0 C_e) + (\mu_0 \mu_e + 1)(C_0 + C_e)C$
$C = \cos\theta$
$C_0 = \cos\theta_0$
$C_e = \cos\theta_e$.

If we assume that the transmitting antenna has a cosinusoidal pattern in elevation over a perfectly reflecting ground, the radiation field is given by

$$E_{||} = K\sqrt{P}\cos\beta, \qquad (6)$$

where $E_{||}$ = the normal or parallel field component,
K = a constant of proportionality,
P = the radiated power in kw,
β = the elevation angle at the ground.

The response of a loop antenna over a highly conducting ground in terms of the electric field [Crary, 1961] is

$$v_L = h'_L(E_{||}\cos\phi - E_{\perp}\sin\phi\sin\beta), \qquad (7)$$

where v_L = the induced voltage in the loop,
h'_L = the effective height of the loop over a highly conducting ground,
ϕ = the angle between the plane of the loop and the plane of incidence.

The abnormal loop response is then given by

$$v_A = \frac{K\sqrt{P}\cos\beta\ {}_{||}R_{\perp}\sin\beta}{P_n}, \qquad (8)$$

and the normal loop response is given by

$$v_N = \frac{K\sqrt{P}\cos\beta_{||}R_{||}}{P_n}. \tag{9}$$

The night to day amplitude ratios, $A_{||N}/A_{||D}$ and $A_{\perp N}/A_{\perp D}$, are then found from (8) and (9) to be

$$\frac{A_{||N}}{A_{||D}} = \frac{\cos\beta_{N||}R_{||N}P_D}{\cos\beta_{D||}R_{||D}P_N} \tag{10}$$

and

$$\frac{A_{\perp N}}{A_{\perp D}} = \frac{\sin\beta_N\cos\beta_{N||}R_{\perp N}P_D}{\sin\beta_D\cos\beta_{D||}R_{\perp D}P_N}. \tag{11}$$

8. References

Appleton, E. V. (1953), A note on the "sluggishness" of the ionosphere, J. Atmospheric Terrest. Phys. **3,** 282–284.

Best, J. E., J. A. Ratcliffe, and M. V. Wilkes (1936), Experimental investigation of very long waves reflected from the ionosphere, Proc. Roy. Soc. **A156,** 614–633.

Billings, D. E., D. E. Trotter, and W. E. LaVelle (July 26, 1963), Preliminary report of solar activity, TR No. 621, High Altitude Observatory, University of Colorado, Boulder, Colo.

Bracewell, R. N., and T. W. Straker (1949), The study of solar flares by means of very long radio waves, Monthly Notices, Roy. Astron. Soc. **109,** 28–45.

Bracewell, R. N. (1952), Theory of formation of an ionospheric layer below the *E* layer based on eclipse and solar flare effects at 16 ks, J. Atmospheric Terrest. Phys. **2,** 226–235.

Bracewell, R. N., K. G. Budden, J. A. Ratcliffe, T. W. Straker, and K. Weekes (1951), The ionospheric propagation of low and very low frequency radio waves over distances less than 1000 km, Proc. IEE III **98,** 221–236.

Budden, K. G. (1951), The reflection of very low frequency radio waves at the surface of a sharply bounded ionosphere with superimposed magnetic field, Phil. Mag. **42,** 833–850.

Budden, K. G. (1953), The propagation of very low frequency waves to great distances, Phil. Mag. **44,** 504–513.

Crain, C. M. (1961), Ionization loss rates below 90 km, J. Geophys. Res., **66,** No. 4, 1117–1126.

Crary, J. H. (1961), The effect of the earth-ionosphere waveguide on whistlers, Tech. Rpt. No. 9, Radioscience Laboratory, Stanford University, Stanford, Calif.

CRPL–F Series (1963), Solar Geophysical Data, Part B.

Friedman, H. (1963), Ultraviolet and x-rays from the sun, Annual Review of Astronomy and Astrophysics **1,** 59–96, L. Goldberg, ed. Annual Reviews, Inc., Palo Alto, Calif.

Gallet, R. M. (1955), private communication.

Helliwell, R. A. (Feb. 1953), Graphical solution of skywave problems, Electronics, 150–152.

Lerfald, G. M., J. K. Hargreaves, and J. M. Watts (1965), *D* region absorption at 10 and 15 Mc/s during the total solar eclipse of July 20, 1963, Radio Sci. J. Res. NBS **69D,** No. 7.

Minnis, C. M. (1955), Ionospheric behaviour at Khartoum during the eclipse of 25 February 1952, J. Atmospheric Terrest. Phys. **6,** 91–112.

Mitra, A. P., and R. E. Jones (1954), Recombination in the lower ionosphere, J. Geophys. Res. **59,** 391–406.

Nicolet, M., and A. C. Aikin (1960), The formation of the *D* region of the ionosphere, J. Geophys. Res. **65,** 1469–1483.

Ratcliffe, J. A. (1956), A survey of solar eclipses and the ionosphere, in Solar Eclipses and the Ionosphere **6,** of Special Supplements to J. Atmospheric Terrest. Phys. (Pergamon Press, London).

Reid, G. C. (1964), Physical processes in the *D* region of the ionosphere, Rev. Geophys. **2,** 311–333.

Wait, J. R., and A. Murphy (1956), Multiple reflections between the earth and the ionosphere in VLF propagation, Geofisica Pura e Applicata **35,** 61–72.

Wait, J. R., and A. Murphy (1957), The geometrical optics of VLF skywave propagation, Proc. IRE **45,** No. 6, 754–760.

Wait, J. R., and L. C. Walters (1963), Reflection of VLF radio waves from an inhomogeneous ionosphere, Part I, Exponentially varying isotropic model, J. Res. NBS **67D** (Radio Prop.), No. 3, 361–367.

(Paper 69D7–528)